

Faculty Scholarship

---

5-26-2023

## Inhibition of Wnt/ $\beta$ -Catenin Pathway Overcomes Therapeutic Resistance to Abiraterone in Castration-Resistant Prostate Cancer

Ibrahim M. Atawia  
*Case Western Reserve University*

Prem P. Kushwaha  
*Case Western Reserve University, ppk22@case.edu*

Shiv Verma  
*Case Western Reserve University, sxv304@case.edu*

Spencer Lin  
*Case Western Reserve University, syl35@case.edu*

Eswar Shankar  
*Case Western Reserve University*

*See next page for additional authors*  
Follow this and additional works at: <https://commons.case.edu/facultyworks>



Part of the [Medicine and Health Sciences Commons](#)

---

### Recommended Citation

Atawia IM, Kushwaha PP, Verma S, et al. Inhibition of Wnt/ $\beta$ -catenin pathway overcomes therapeutic resistance to abiraterone in castration-resistant prostate cancer. *Molecular Carcinogenesis*. 2023;62:1312-1324. doi:10.1002/mc.23565

This Article is brought to you for free and open access by Scholarly Commons @ Case Western Reserve University. It has been accepted for inclusion in Faculty Scholarship by an authorized administrator of Scholarly Commons @ Case Western Reserve University. For more information, please contact [digitalcommons@case.edu](mailto:digitalcommons@case.edu).


CWRU authors have made this work freely available. [Please tell us](#) how this access has benefited or impacted you!

---

**Authors**

Ibrahim M. Atawia, Prem P. Kushwaha, Shiv Verma, Spencer Lin, Eswar Shankar, and Sanjay Gupta

# Inhibition of Wnt/ $\beta$ -catenin pathway overcomes therapeutic resistance to abiraterone in castration-resistant prostate cancer

Ibrahim M. Atawia<sup>1,2</sup> | Prem P. Kushwaha<sup>1,3</sup> | Shiv Verma<sup>1,3</sup> | Spencer Lin<sup>4</sup> |  
Eswar Shankar<sup>1,3</sup> | Osama Abdel-Gawad<sup>2</sup> | Sanjay Gupta<sup>1,3,5,6,7,8</sup> 

<sup>1</sup>Department of Urology, Case Western Reserve University, Cleveland, Ohio, USA

<sup>2</sup>Department of Urology, Menoufia University, Menoufia, Egypt

<sup>3</sup>University Hospitals Cleveland Medical Center, The Urology Institute, Cleveland, Ohio, USA

<sup>4</sup>College of Arts and Sciences, Case Western Reserve University, Cleveland, Ohio, USA

<sup>5</sup>Department of Pharmacology, Case Western Reserve University, Cleveland, Ohio, USA

<sup>6</sup>Department of Pathology, Case Western Reserve University, Cleveland, Ohio, USA

<sup>7</sup>Department of Nutrition, Case Western Reserve University, Cleveland, Ohio, USA

<sup>8</sup>Case Comprehensive Cancer Center, Division of General Medical Sciences, Cleveland, Ohio, USA

## Correspondence

Sanjay Gupta, Department of Urology, Case Western Reserve University 10900 Euclid Ave, Cleveland, Ohio 44106, USA.  
Email: [sanjay.gupta@case.edu](mailto:sanjay.gupta@case.edu)

## Funding information

U.S. Department of Defense

## Abstract

Abiraterone acetate has been clinically approved for the treatment of patients with advanced-stage prostate cancer. It reduces testosterone production by blocking the enzyme cytochrome P450 17 alpha-hydroxylase. Despite improved survival outcomes with abiraterone, almost all patients develop therapeutic resistance and disease recurrence, progressing to a more aggressive and lethal phenotype. Bioinformatics analyses predicted activation of canonical Wnt/ $\beta$ -catenin and involvement of stem cell plasticity in abiraterone-resistant prostate cancer. Increased expression of androgen receptor (AR) and  $\beta$ -catenin and their crosstalk causes activation of AR target genes and regulatory networks for which overcoming acquired resistance remains a major challenge. Here we show that co-treatment with abiraterone and ICG001, a  $\beta$ -catenin inhibitor, overcomes therapeutic resistance and significantly inhibited markers of stem cell and cellular proliferation in abiraterone-resistant prostate cancer cells. Importantly, this combined treatment abrogated the association between AR and  $\beta$ -catenin; diminished SOX9 expression from the complex more prominently in abiraterone-resistant cells. In addition, combined treatment inhibited tumor growth in an in vivo abiraterone-resistant xenograft model, blocked stemness, migration, invasion, and colony formation ability of cancer cells. This study opens new therapeutic opportunity for advanced-stage castration-resistant prostate cancer patients.

## KEYWORDS

androgen deprivation therapy, androgen receptor, cancer stem cells, castration resistant prostate cancer, signaling pathways

**Abbreviations:** APC, adenomatous polyposis coli; AR, androgen receptor; CRPC, castration-resistant prostate cancer; DEGs, differentially expressed genes; GSK3, glycogen synthase kinase 3; PSA, prostate specific antigen; Wnt, wingless-related integration sites.

Ibrahim M. Atawia and Prem P. Kushwaha contributed equally to this study.

This is an open access article under the terms of the Creative Commons Attribution-NonCommercial-NoDerivs License, which permits use and distribution in any medium, provided the original work is properly cited, the use is non-commercial and no modifications or adaptations are made.

© 2023 The Authors. *Molecular Carcinogenesis* published by Wiley Periodicals LLC.

## 1 | INTRODUCTION

Abiraterone acetate (Zytiga<sup>®</sup>) is a second-generation antiandrogen approved by the Food and Drug Administration for the treatment of hormone naïve and metastatic castration-resistant prostate cancer (CRPC).<sup>1,2</sup> In contrast to canonical antiandrogens that targets androgen receptor (AR), abiraterone acetate is a selective inhibitor of CYP17A1 that inhibits androgen production in the testes and adrenal glands.<sup>1-3</sup> Multiple randomized clinical trials have shown significant improvement of >50% decline in prostate-specific antigen (PSA) and time to PSA progression with abiraterone acetate leading to prolonged overall survival in CRPC patients.<sup>4,5</sup> However, abiraterone-resistant CRPC has become a common and major challenge in the management of abiraterone-resistant phenotype. Majority of abiraterone-resistant prostate tumors have demonstrated an association between canonical Wntless-related integration sites (Wnt)/ $\beta$ -catenin pathway genes and reduced PSA-free survival. Whole exome sequencing analysis demonstrated a large number of patients on abiraterone-prednisone therapy developed resistance due to mutations in the Wnt/ $\beta$ -catenin pathway.<sup>6</sup> These activating mutations in the Wnt pathway were two times higher in patients that did not respond to abiraterone-prednisone treatment, compared to the responders. Another study on RNA-sequencing of circulating tumor cells implicated noncanonical Wnt pathway activation in response to antiandrogens.<sup>7</sup> A large-scale sequencing effort in biopsy or at rapid autopsy have discovered genomic aberrations in the Wnt signaling pathway in approximately 20% metastatic CRPC tumors.<sup>8</sup>

The canonical and noncanonical Wnt signaling pathway regulates several developmental and biological processes including, cell proliferation, self-renewal, and stem cell differentiation.<sup>9,10</sup> In noncanonical signaling pathway, Wnt5a, Wnt5b, and Wnt11 ligands bind to a panel of diverse receptors to activate Wnt signaling, including receptors of the Frizzled family and other mediators such as tyrosine-protein kinase transmembrane receptor (ROR1, ROR2, or RYK). Binding of these noncanonical Wnt ligands can activate multiple intracellular pathways including the planar cell polarity and calcium signaling pathways.<sup>11-13</sup> The canonical Wnt signaling is dependent on  $\beta$ -catenin as an effector of Wnt proteins, and its high level induces tumorigenesis.<sup>14,15</sup> In the absence of extracellular Wnt signals, cytoplasmic  $\beta$ -catenin is phosphorylated by glycogen synthase kinase 3 (GSK3) as part of a destruction complex including adenomatous polyposis coli (APC) and axin proteins. The phosphorylated  $\beta$ -catenin is then ubiquitinated and degraded. Wnt signaling inhibits this process leading to the accumulation of  $\beta$ -catenin in the nucleus by enabling the formation of transcriptionally active complexes. Interaction of  $\beta$ -catenin and its crosstalk with AR has been well documented in prostate cancer.<sup>16,17</sup> AR binds  $\beta$ -catenin directly to stimulate AR-mediated gene transcription that provide growth advantage engaging downstream targets such as c-Myc and cyclin D1, even at the castration levels of androgens.<sup>18</sup> Studies have shown that SOX-9, a transcription factor, regulates the interaction between AR and  $\beta$ -catenin as a critical factor in prostate cancer.<sup>19,20</sup> Growing evidence shows that Wnt/ $\beta$ -catenin signaling has been

critical for cancer cell differentiation and is highly active in cancer stem-like cells, primarily responsible for the emergence of abiraterone-resistant phenotype.

In this study, we determine whether inhibition of  $\beta$ -catenin would repress prostate cancer growth and overcome abiraterone resistance by disrupting both AR and Wnt/ $\beta$ -catenin signaling. Targeting canonical Wnt signaling through  $\beta$ -catenin could be an important therapeutic strategy to delay the development of abiraterone resistance in CRPC cells.

## 2 | MATERIALS AND METHODS

### 2.1 | Materials

$\beta$ -catenin inhibitor ICG001 (Cat# A11039) and abiraterone acetate (Cat# CB7630) were purchased from Adooq Bioscience LLC. Antibodies including anti-AR (Cat# 5153S), anti-PSA (Cat# 2475S), anti- $\beta$ -catenin (Cat# 9562), anti-CDC20 (Cat# 4823), anti-SOX-9 (Cat# 82630T), anti-OCT-4 (Cat# 75463) and GSK3 $\beta$  (Cat# 9332) were purchased from Cell Signaling Technologies (Danvers MA). Anti-PCNA (Cat# sc-56), anti-SOX-2 (Cat# sc-20088), anti-ALDH1 (Cat# sc-166362), and anti-GAPDH (Cat# sc-365062) antibodies were purchased from Santa Cruz Biotechnology (Dallas, TX). Anti-cyclin D1 (Cat# NBP2-15189) and anti-c-Myc (Cat# sc-40) antibodies were purchased from Enzo Life Sciences.

### 2.2 | Patient data

The gene expression data GEO (accession# GSE102124) was analyzed in the study that consists of control (untreated) specimens of primary prostate cancer ( $n=3$ ) and prostate cancer specimens treated with neoadjuvant androgen deprivation therapy (abiraterone acetate plus prednisone for >6 months;  $n=19$ ). Transcriptome analyses were performed on laser capture microdissected foci of residual tumors from these patients. For gene expression analysis Human Transcriptome Array 2.0, GPL17587-HTA-2\_0 (GeneChip™ Human Transcriptome Array 2.0) platform was used that comprised of >245,000 coding transcripts, and in total, 70,524 transcripts for both coding and noncoding regions.

### 2.3 | Cell culture

Androgen-responsive human prostate cancer LNCaP and C4-2B cells were grown in RPMI1640 (Cat# SH30027.01, GE Healthcare) supplemented with 10% fetal bovine serum, 50 U/mL penicillin and 50  $\mu$ g/mL streptomycin in 100-mm tissue culture plates at 37°C in a humidified atmosphere (5% CO<sub>2</sub>). LNCaP cells are derived from a needle biopsy taken from the left supraclavicular lymph node metastasis that harbors AR point mutation containing the threonine to alanine mutation of amino acid 877.<sup>21</sup> This mutation has been

observed in both naïve and CRPC patients. C4-2B cells are derivative of LNCaP cells, procured from bone metastasis in nude mice and is considered a useful preclinical model for metastatic, castration-resistant and androgen receptor-positive prostate cancer having distinct genomic and transcriptomic profiles.<sup>22</sup> These cells were used for generating abiraterone-resistant clones by exposing to 20  $\mu$ M abiraterone acetate for a minimum of 6 months and maintaining in media containing 5  $\mu$ M abiraterone acetate. Under the conditions, both cell lines underwent morphological changes such as loss of cell-to-cell tight contact with scattered growth and temporary arm-like projections. The growth curves for both cell lines demonstrate a marked difference in their sensitivity to abiraterone treatment (Supporting Information: Figure S1). The absence of mycoplasma contamination was tested using PCR-based assay (Cat# MP0025; Sigma-Aldrich). The parental cells were maintained in the drug vehicle for the same time period and served as corresponding controls.

## 2.4 | Alkaline phosphatase staining

C4-2B abiraterone-resistant and parental cells were stained for alkaline phosphatase activity as a measure of pluripotency using alkaline phosphatase live stain reagent (Cat# A14353; Thermo Fisher Scientific). The dye is a nontoxic, cell-permeable fluorescent substrate for alkaline phosphatase that diffuses out over the course of 2 h. The cells were incubated with the substrate for 30 min and washed twice with RPMI1640 culture media to remove excess reagent. Following the final wash, fresh media was added, and images were captured within 30–60 min after staining. Visualization of fluorescent-labeled cells were observed under fluorescent microscopy using a standard FITC filter as previously described.<sup>23</sup>

## 2.5 | Library preparation and next generation sequencing

Total RNA was extracted from both C4-2B abiraterone-resistant and parental cells continuously exposed to 5  $\mu$ M abiraterone using RNA RNeasy kit (Qiagen). The total RNA integrity (RIN) was assessed using an RNA 6000 nanochip (Agilent Technologies) on a Bioanalyzer 2100 (Agilent Technologies). Libraries were prepared using the Illumina TruSeq Stranded Total RNA Sample Preparation kit according to the manufacturer's protocol. The 50 bp single-end sequencing was performed on pooled libraries using an Illumina HiSeq. 2500 platform. Library preps and sequencing were completed by the Case Western Reserve University Genomics Core Facility.

## 2.6 | Next generation sequencing data analysis

Sequencing reads generated from the Illumina platform were assessed for quality using FastQC. Illumina HiSeq. A total of 2500 reads were trimmed and clipped for quality control in TrimGalore

v0.4.3 a wrapper script for cutAdapt and FastQC. Alignment of the data was performed using STAR Aligner v2.5.3 using the human reference genome GRCh38 and the GENCODE transcript annotation v25. Differential gene expression was determined using Cufflinks v2.2.1. Differentially expressed genes (DEGs) were identified using multiple testing corrected  $q < 0.05$ . Mitochondrial chromosomes and the nonchromosomal sequences were excluded from the analysis. The Next-Gen sequencing data of C4-2B abiraterone-resistant cells were submitted to NCBI-GEO having accession number GSE220467.

## 2.7 | Pathway and gene set enrichment analysis

To evaluate the gene set analysis performance, gene expression data was analyzed for enrichment using GSEA software (Broad Institute-version 2.2.0) and MSigDB version 5.1 that calculates a normalized enrichment score indicating any overrepresentation of predefined gene set in response to treatment, compared to control.<sup>24</sup> The gene set collections obtained were annotations of signaling pathways (BioCarta, KEGG, and Reactome), Gene Ontology annotations (biological process, molecular function, cellular compartment), and Human Phenotype Ontology (HPO—human only). Pathway analysis was performed using Ingenuity Pathway Analysis v 5.0 (IPA; Qiagen), the DEGs were imported into the IPA software and were subjected to functional annotations and regulatory network analysis. The DEGs were overlaid with ingenuity knowledge database of humans, and, to evaluate the definite overrepresented pathway(s), or to remove the chances of any randomness in data with reference to  $p$  value, another statistical parameter of a threshold value of 0.05 and Benjamin-Hochberg (B-H) was applied and represented in the form of bar graph, with the scale of gene and  $-\log$  (B-H  $p$  value).

## 2.8 | Quantitative real-time PCR

Total RNA was isolated from abiraterone-resistant and parental cells, and RNA quality was analyzed using NanoDrop ND-1000 Spectrophotometer (NanoDrop). One microgram total RNA was used for cDNA synthesis (Applied Biosystems™) using High-Capacity cDNA Reverse Transcription Kit (Thermo Fisher). To quantify and amplify the gene oligonucleotides designed by Integrated DNA Technologies were used. The list of genes probed are mentioned in Supporting Information: Table 1, GAPDH (NM\_008084), and Actin (NM\_007393) were used as internal controls in the reaction. All reactions were performed in triplicate (three biological and three technical replicates) along with no template controls. The reaction for qRT was setup accordingly; 2.5  $\mu$ L of SYBR green (Radiant™ SYBR Green low-ROX qPCR, Alkali Scientific) of 5x sample were added for a total 10  $\mu$ L volume with thermal cycler program used started at 50°C for 2 min then proceeded with 95°C for 10 min for initial denaturing, followed by 40 cycles of 95°C for 15 s, 60°C for 40 s, and 72°C for 35 s to collect cycle threshold ( $C_t$ ) values, along with dissociation curve cycle. The  $2^{-\Delta\Delta C_t}$  method was used to calculate relative expression of each gene as previously described.<sup>23</sup>

## 2.9 | MTT assay

Cell viability was assessed using 3-(4,5-dimethylthiazol-2-yl)-2,5-diphenyltetrazolium bromide (MTT) (Cat# M6494, Thermo Fisher Scientific) reagent. To determine the individual efficacy of ICG001 and abiraterone, C4-2B abiraterone-resistant and parental cells were propagated in 96 well plates at a density of  $2 \times 10^3$ /well in RPMI1640 with 10% FBS medium; allowed to incubate at 37°C in a 5% CO<sub>2</sub> environment. Cells were treated with various concentrations of ICG001 and abiraterone for 24 h followed by addition of 10 µL of MTT reagent (5 mg/mL) to each well and incubated at 37°C for 3 h. The reaction was terminated by adding 100 µL of DMSO to dissolve the crystals formed. The absorbance was measured at 590 nm on a plate reader. The percentage of cell viability was determined in comparison to the control. In the subsequent experiment, the C4-2B abiraterone-resistant and parental cells were treated with a combination of ICG001 and abiraterone for 24 h. The percentage inhibition was calculated to determine the ratio that caused maximum inhibition.

## 2.10 | Colony formation assay

For anchorage-independent cell growth, a soft agar colony formation assay was performed in a six-well plate (Costar-Corning Incorporated). Each well contained 2 mL of 0.5% agar in the medium as the bottom layer, 1 mL of 0.38% soft agar (Sigma) in the medium, and ~2000 cells at the feeder layer treated individually and in combination with ICG001 and abiraterone acetate in culture medium. Cultures were maintained at 37°C in a humidified 5% CO<sub>2</sub> atmosphere. The number of colonies were determined after 2 weeks by counting them under an inverted phase-contrast microscope at ×400 magnification and a group of ~20 cells was counted as a colony.

## 2.11 | Wound healing assay

C4-2B abiraterone-resistant and parental cells were seeded at 70%–80% confluence into six-well culture plates. After the cells grew to confluence, using a sterile pipette tip, at least three scratch wound per plate was made. The cell monolayer was washed once with 1× phosphate-buffered saline (PBS) to remove any floating cells, following treatment individually and in combination with ICG001 and abiraterone acetate. The plates were incubated at 37°C in a 5% CO<sub>2</sub> humidified incubator and photographed at indicated time points. Cell migration areas were calculated using Image J software as previously described.<sup>25</sup>

## 2.12 | Invasion assay

Invasion assay was performed as previously described.<sup>25</sup> Briefly, 24-well ThinCert cell culture inserts 8 µM pore size was purchased

from Greiner-Bio One, Monroe, NC (Cat #662638) to study the anti-invasive effect of ICG001 and abiraterone acetate and their combination on C4-2B abiraterone-resistant and parental cells. The inserts were coated with 100 µL (1 mg/mL) Matrigel (Cat #3433-001-R1; TREVIGEN). After coating, the inserts were incubated at 37°C in a CO<sub>2</sub> incubator for 1 h before being used. Cells were serum starved for 24 h following which was trypsinized and resuspended in serum-free media. The cells were counted, and  $5 \times 10^4$  cells/mL was added to the upper chamber containing the vehicle, ICG001 and abiraterone acetate and their combination and the lower chamber was replenished with RPMI1640 containing 10% FBS. Following treatment, the cells were incubated for 48 h in the CO<sub>2</sub> incubator at 37°C. After 48 h, noninvasive cells, and the gel in the upper compartment of the inserts were removed with a cotton swab moisturized with double distilled H<sub>2</sub>O. The invasive cells in the lower chamber were fixed with 3.7% formaldehyde for 2 min and washed with PBS; permeabilized with methanol and stained with 0.5% crystal violet. The wells were washed with PBS to remove excess crystal violet followed by addition of 1% Triton to each membrane. The chambers were incubated, and the eluent was read at 480 nm using a plate reader. The difference in absorbance represented the effect of compounds on the invading cells. The percentage of invasion was calculated and represented as a bar graph.

## 2.13 | Cell cycle analysis

C4-2B abiraterone-resistant and parental cells were serum starved for 24 h to synchronize and treated with the indicated concentrations of ICG001 and abiraterone acetate individually and in combination for 24 h. The cells were trypsinized, washed twice with cold 1 × PBS, fixed and permeabilized with 90% cold methanol overnight at –20°C. The cells were then incubated at 37°C with 20 µg/mL RNase A in 1 × PBS for 30 min and stained with 50 µg/mL propidium iodide for 30 min. The samples were analyzed using an Epics XL cytometer (Beckman Coulter), EXPO32 acquisition software (version 12; Verity Software), and WinList analysis software (version 7; Verity Software).

## 2.14 | Western blotting

Total cell and tumor lysates from treated and untreated groups were prepared as described previously.<sup>25</sup> Forty micrograms protein was denatured at 95°C and resolved on a 4%–20% SDS–PAGE gel (Bio-Rad). The gels were transferred to a nitrocellulose membrane, blocked with 5% nonfat dry milk TBST, pH 7.4 for 1 h, and the membrane was probed with primary antibody overnight at 4°C overnight. The following day the blots were incubated with corresponding HRP-conjugated secondary antibody (Santa Cruz Biotechnology), and detected using ECL reagent (Cat# XR93, Alkali Scientific Inc). The bands were visualized on autoradiography film (Cat# XR1570, Alkali Scientific Inc).



## 2.15 | Immunoprecipitation assay

C4-2B abiraterone-resistant and parental cells were grown in 100 mm dishes, allowed to attach overnight. The following day, the cells were treated with the indicated concentrations of ICG001 and abiraterone acetate individually and in combination for 24 h. Lysates of treated and untreated cells were prepared using RIPA buffer (Cat# 9806, Cell Signaling Technologies). 200 µg of protein was immunoprecipitated with 2 µg AR antibody (Cat# SC-7305, Santa Cruz Biotech) at 4°C for 3 h. Twenty microliter protein A/G agarose beads (Cat# SC-2003, Santa Cruz Biotech) were added and incubated overnight at 4°C. Immunoprecipitated proteins were washed totally four times, two times with 1x RIPA lysis buffer and two times with 1x cold PBS, following which 50 µL of 1x SDS loading buffer was added to elute the proteins at 50°C for 10 min. The samples were centrifuged at 6000 rpm at room temperature for 5 min and 30 µL of the upper layer of the supernatant was electrophoresed by SDS-PAGE and analyzed by Western blotting as previously described.<sup>25</sup> Two hundred micrograms of protein from each group was also processed with IgG and the beads; eluted as controls and loaded in the gel. Western Blotting was performed on a portion of the lysate that was boiled in 4x SDS and loaded as input and probed for AR, β-catenin, and SOX9 antibodies.

## 2.16 | Animal studies

Animal experiments using male NCr-nu/nu mice were performed in accordance with recommendations of the Guide for the Care and Use of Laboratory Animals of the NIH, and protocol was approved by the CWRU School of Medicine Institutional Animal Care and Use Committee. After C4-2B abiraterone-resistant cells ( $2.5 \times 10^5$  cells per mouse/flank) were inoculated into both the flanks of nude mice for 2 weeks, animals were randomized into treatment and control groups of six mice each, followed by oral gavage of abiraterone acetate suspension in vehicle 5 days per week. The ICG001 suspension was prepared in vehicle and provided to mice thru oral gavage twice weekly. Tumor wet weight (g) and volumes were calculated from the formula  $V = L \times W^2/2$  [where V is a volume ( $\text{mm}^3$ ), L is length (mm), and W is the width (mm)].

## 2.17 | Statistical analysis

Statistical analysis was performed using two-tailed Student's *t* test. Association for pathways connected with abiraterone resistance was conducted with  $\chi^2$  or Fisher exact tests.  $p < 0.05$  was considered statistically significant. The level of significance designated statistically significant are as follows: \* $p \leq 0.05$ , \*\* $p \leq 0.01$ , \*\*\* $p \leq 0.001$ .

## 3 | RESULTS

The gene expression analysis between abiraterone-treated and untreated patients were compared. A total of 7533 differentially expressed genes (DEGs) that include 5537 upregulated and 1996 downregulated genes were mapped, analyzed, and displayed in a volcano plot representing the gene expression change (log<sub>2</sub> fold-change; x-axis) and statistical significance of change (-log<sub>10</sub> adjusted *q* value; y-axis). The dots in the volcano plot represent individual gene transcripts expressed differentially between abiraterone-treated and untreated patients at  $p_{\text{adj}} < 0.05$  (Figure 1A). To identify the signaling pathways associated with abiraterone resistance, the Ingenuity Pathway Analysis (IPA) was performed followed by setting of the statistical parameters using the Fisher exact test *p* value, -log ( $p > 3$ ), and the threshold value of 0.05. The analysis identified Wnt/β-catenin pathway, NANOG signaling, Wnt/GSK3β, TGF-β, OCT4 pathway, autophagy, and glycogen degradation II as abiraterone-canonical signaling pathways, whereas Wnt/Ca<sup>2+</sup> signaling was identified as a noncanonical Wnt pathway (Figure 1B). In addition, DEGs with gene set enrichment analysis (GSEA) between abiraterone-treated and untreated patients were constructed (Supporting Information: Table S2). The GSEA plots from BIOCARTA, Hallmark, and GOBP demonstrated significant gene enrichment and overrepresentation of the positive regulation of the canonical Wnt/β-catenin signaling pathway at a threshold of FDR  $p < 0.05$  (Figure 1C).

In the next set of experiments, both C4-2B and LNCaP abiraterone-resistant cells and their parental counterparts were treated with abiraterone and ICG001 to determine the sensitivity of exposure. Treatment with 5–20 µM abiraterone acetate resulted in 8%–20% decrease in cell viability in C4-2B abiraterone-resistant cells and 23%–52% in C4-2B parental cells. Similar trend was noted in LNCaP cells where treatment with 5–20 µM abiraterone acetate resulted in 12%–28% decrease in cell viability in LNCaP abiraterone-resistant cells and 58%–89% in LNCaP parental cells (Supporting Information: Figure S2). The IC<sub>50</sub> values of ICG001 and abiraterone in C4-2B abiraterone-resistant cells were 2.1 and >100 µM, whereas in C4-2B parental cells the IC<sub>50</sub> values were >10 and 22 µM, respectively. In LNCaP abiraterone-resistant cells, the IC<sub>50</sub> values of ICG001 and abiraterone were 1.4 and >80 µM, whereas in LNCaP parental cells the IC<sub>50</sub> values were >12 and 6.4 µM (Supporting Information: Figure S2). The growth curves for both cell lines demonstrated a similar trend of difference in their sensitivity to abiraterone and ICG001 treatment, therefore we elected to use C4-2B abiraterone-resistant cells and their parental counterpart for additional experiments.

We next performed Ingenuity Pathway Analysis (IPA) and knowledge database on DEGs to investigate the biological relevance and pathway association of C4-2B abiraterone-resistant cells and compared with the parental counterpart. A total of 5977 DEGs were analyzed using IPA. The analysis exhibited 3112 upregulated and 2865 downregulated DEGs in C4-2B abiraterone-resistant cells (data not shown). Moreover, the result of heat map analyzed through

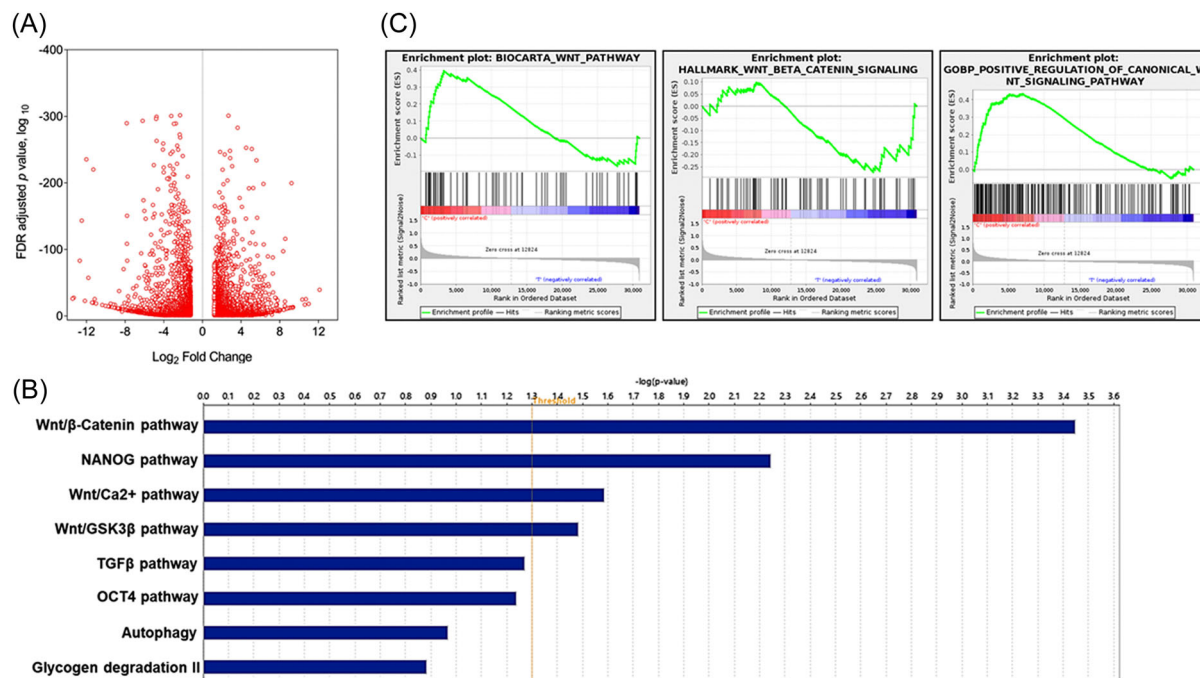


**FIGURE 1** Systematic transcriptomic comparison between abiraterone treated and untreated prostate cancer patients. (A) Volcano plot represents individual gene transcripts expressed differentially between abiraterone-treated and untreated patients at  $p$  adj < 0.05. (B) Signaling pathways associated with abiraterone resistance. The ingenuity pathway analysis (IPA) was performed followed by setting of the statistical parameters using the Fisher exact test  $p$  value,  $-\log(p > 3)$ , and the threshold value of 0.05. (C) Gene set enrichment analysis (GSEA) between abiraterone-treated and untreated patients. GSEA plots from BIOCARTA, Hallmark, and GOBP demonstrate significant gene enrichment and overrepresentation of the positive regulation of the canonical WNT/ $\beta$ -catenin signaling pathway at a threshold of FDR  $p < 0.05$ . Details are provided in Section 2.

ingenuity knowledge database revealed HIF-1 signaling pathway, Wnt signaling, adherens junction, arginine biosynthesis, glycolipid metabolism as few top pathways significantly overexpressed in abiraterone-resistant cells, compared to untreated cells (Figure 2A). The resistant cell line demonstrated changes in the Wnt/ $\beta$ -catenin pathway as the most highly enriched pathway during abiraterone-resistance. The GSEA plots from GO, HALLMARK, and REACTOME demonstrated significant gene enrichment of both Wnt/ $\beta$ -catenin canonical and noncanonical Wnt pathway altered at a threshold of FDR  $p < 0.05$  (Figure 2B).

To identify candidate genes that confer resistance to abiraterone, we performed quantitative-PCR on a subset of genes belonging to both canonical and noncanonical Wnt/ $\beta$ -catenin signaling pathway, cancer stem cell markers and downstream targets of  $\beta$ -catenin such as c-Myc, Cyclin D1, and CDC20 using C4-2B abiraterone-resistant and parental cell line. A significant increase in the Log<sub>2</sub> relative expression of canonical Wnt signaling (WNT2B, WNT3, and WNT3A) and WNT5A, a noncanonical Wnt signaling ligand was observed in abiraterone-resistant cells, compared to parental cells. In addition, a modest increase in SOX2 and OCT4 expression was observed, whereas a significant increase in Log<sub>2</sub> relative expression was noted in ALDH1, SOX9,  $\beta$ -catenin, c-Myc, Cyclin D1, and CDC20 in abiraterone-resistant cells, compared to parental cells (Figure 2C).

Since  $\beta$ -catenin is highly upregulated in abiraterone-resistant cells, we tested the effect of its inhibitor, ICG001 on cell viability in

combination with abiraterone acetate. Exposure of C4-2B abiraterone-resistant cells ranging from 1 to 4  $\mu$ M concentration of ICG001 alone resulted in 27%–78% decrease in cell viability. The results obtained in C4-2B parental cells showed approximately 8%–19% decrease in cell viability post-ICG001 exposure at similar concentrations. However, combination treatment with ICG001 and abiraterone at 2 and 20  $\mu$ M (1:10 M ratio) exhibited effective cell growth inhibition of 95%, showing higher sensitivity toward ICG001 exposure in C4-2B abiraterone-resistant cells, compared to 62% cell growth inhibition in C4-2B parental cells (Figure 3A,C). In addition, we evaluated drug ineffectiveness in C4-2B abiraterone-resistant cells and its association with the induction of stem-like characteristics and plasticity, as individual and combination treatments of ICG001 and abiraterone acetate in both cell types. We performed staining of live cells with fluorescence-tagged alkaline phosphatase, as a benchmark for identifying pluripotent stem cells.<sup>26,27</sup> The live stain of abiraterone-resistant cells demonstrates increased number and intensity of alkaline phosphatase positive cells, compared to parental cell lines. Higher intensity of alkaline phosphatase staining along with greater sensitivity toward ICG001 was noted in C4-2B abiraterone-resistant cells, compared to C4-2B parental cells (Figure 3B,D).

Next, we performed cell cycle analysis in both C4-2B abiraterone-resistant and parental cells with ICG001 and abiraterone treatment alone and in combination. As shown with representative



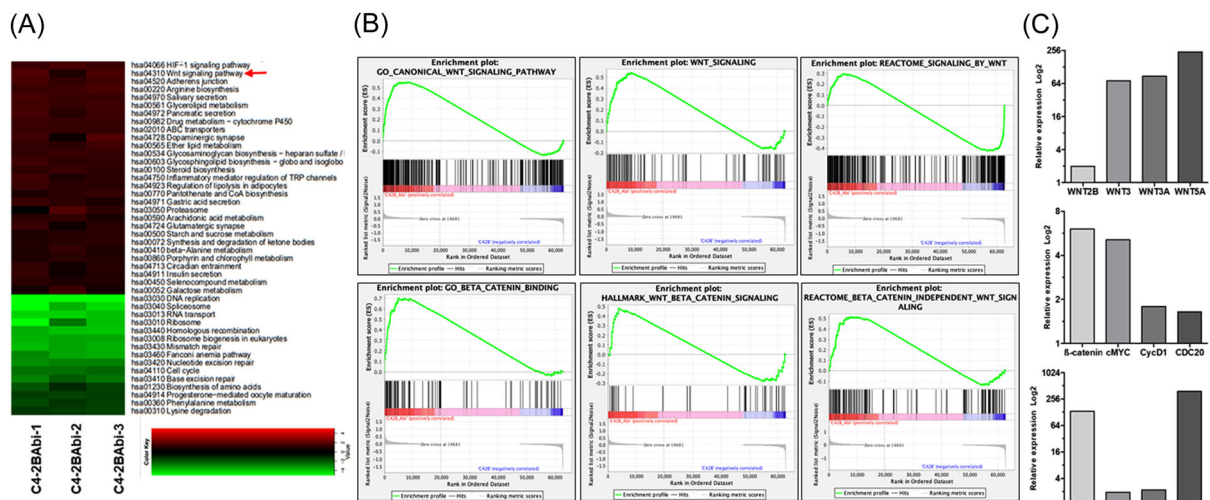


**FIGURE 2** (A) Heat map showing expression of signaling pathways in parental C4-2B, and C4-2B abiraterone-resistant cells exposed to 20  $\mu$ M abiraterone acetate for a minimum of 6 months and maintained in media containing 5  $\mu$ M abiraterone acetate. (B) GSEA plots from GO, HALLMARK, and REACTOME showing significant gene enrichment of the Wnt/ $\beta$ -catenin pathway altered at a threshold of FDR  $p < 0.05$ . (C) Gene transcript belonging to canonical and noncanonical Wnt/ $\beta$ -catenin signaling, cancer stem cell markers and other downstream targets of  $\beta$ -catenin in C4-2B abiraterone-resistant and parental cell line in Log<sub>2</sub> relative expression. Details are provided in Section 2.

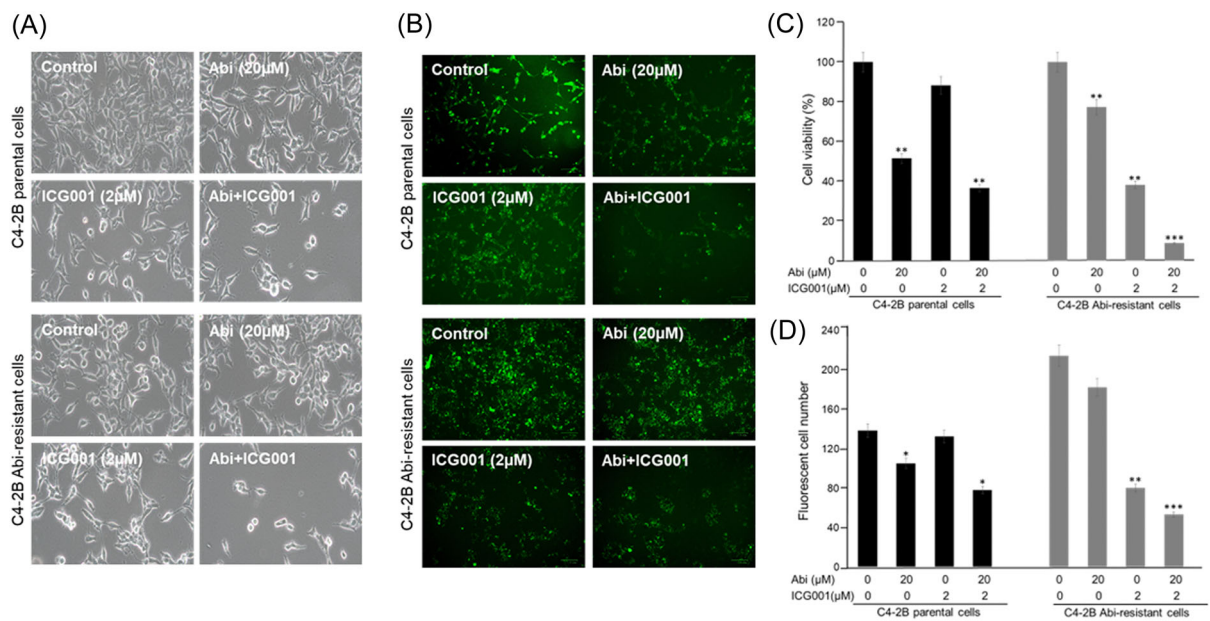


**FIGURE 3** Effect of ICG001 and abiraterone alone or in combination on (A, C) cell viability, (B, D) self-renewal marker expression in pluripotent stem cells. The cells treated with 2  $\mu$ M ICG001 or 20  $\mu$ M abiraterone acetate alone and in combination. The image shows morphological changes and differential staining of cancer stem-like cells in C4-2B parental cells and C4-2B abiraterone-resistant cells. Magnification  $\times 10$ . Flow cytometry was performed following staining with propidium iodide staining. \* $p < 0.05$ , \*\* $p < 0.01$ , \*\*\* $p < 0.001$  versus control. Details are provided in Section 2.

images and bar graph, ICG001 accounted for G1/G0 arrest in both parental and abiraterone-resistant subline (73.4% and 82.3%), whereas abiraterone was mostly active for G1/G0 arrest in the parental cells (63.6% compared to 51.2% in control) and totally ineffective in the abiraterone-resistant subline (58.3% compared to

62.3% in control), as expected from the 6-month selection of its resistance. When the two drugs were combined, ICG001 accounted for the G1/G0 arrest effect solely in the abiraterone-resistant subline (86.2%) and was additive with abiraterone for G1/G0 arrest action in the parental line (78.5%) (Figure 4A,B).

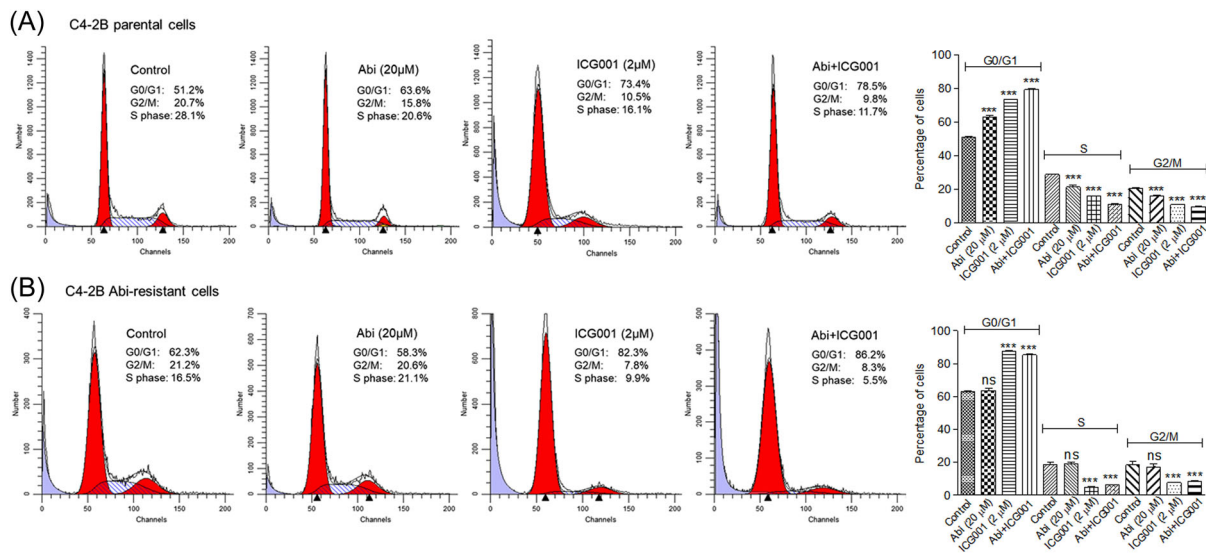


**FIGURE 4** Effect of ICG001 and abiraterone alone or in combination on cell cycle in (A) parental C4-2B and (B) C4-2B abiraterone-resistant cells. The cells treated with 2 µM ICG001 or 20 µM abiraterone acetate alone and in combination. The image shown are representative of each treatment and combination of three replicates of C4-2B parental cells and C4-2B abiraterone-resistant cells. \*\*\* $p < 0.001$  versus control. Details are provided in Section 2.

Evidence suggests that overexpression of  $\beta$ -catenin and AR promote prostate tumorigenesis.<sup>28–30</sup> To investigate if the combination could inhibit cell migration, we performed a wound healing assay. Treatment of C4-2B abiraterone-resistant cells with ICG001 and abiraterone acetate resulted in 59% and 16% decrease in wound closure, compared to untreated cells (45%) at 24 h postexposure. At 48 h, 23% and 65% wound closure were noted with ICG001 in abiraterone-treated cells. In C4-2B parental cells, 2 µM ICG001 and 20 µM abiraterone treatment alone for 24 h caused 48% and 37% decrease in wound closure, compared to 62% in vehicle control cells. The wound closure at 48 h was 55% and 46% in ICG001 and abiraterone treatment groups. Combined treatment with 2 µM ICG001 and 20 µM abiraterone showed marked antimigratory activity causing 8% and 9% wound closure in C4-2B abiraterone-resistant cells and 19% and 38% in C4-2B parental cells after 24 and 48 h treatment. Collectively, this data demonstrates that a combination of 2 µM ICG001 and 20 µM abiraterone treatment decreased migration of abiraterone-resistant cells (Figure 5A,B; Supporting Information: Figure S3).

We next investigated the effect of ICG001 and abiraterone acetate, individually and in combination, on anchorage-independent growth by soft agar colony formation assay. Anchorage-independent growth is one of the hallmarks of malignancy and is direct in vitro assay for detection of malignant transformation of cells.<sup>31</sup> Compared to vehicle-treated controls (seven colonies/field), exposure of C4-2B abiraterone resistant cells to ICG001, abiraterone and their combination resulted in a decrease in anchorage-independent growth and colony formation to 5, 4, and 3 colonies/field. In C4-2B parental cells, exposure with ICG001, abiraterone and their combination resulted in 7, 5,

and 3 colonies/field compared to the 13 colonies/field that were observed in vehicle-treated control (Figure 5C).

To determine whether ICG001 and abiraterone have the ability to influence cancer cell invasiveness, the transwell invasion assay was performed. The test cells invade through the matrigel layer in a comparable manner as they migrate in 2D conditions. Treatment of C4-2B abiraterone-resistant and C4-2B parental cells with ICG001 resulted in 36% and 32% decrease in cell invasion, whereas abiraterone treatment resulted in 16% and 28% inhibition at 24 h postexposure. Combined treatment with 2 µM ICG001 and 20 µM abiraterone showed marked anti-invasive activity resulting in 64% and 40% decrease in cell invasion in C4-2B abiraterone-resistant and C4-2B parental cells after 24 h treatment. Taken together, the results from the invasion assay showed a significant enhancement of the dual combination in the suppression of tumor cell invasion (Figure 5D).

Emerging studies suggest that inhibition of AR pathway results in canonical Wnt/ $\beta$ -catenin activation and cellular plasticity by reciprocal feedback activation.<sup>32,33</sup> Therefore, we subsequently determined the effect of abiraterone and ICG001 alone and in combination on AR, PSA,  $\beta$ -catenin, c-Myc, cyclin D1, GSK3 $\beta$ , CDC20, ALDH1, SOX2, and OCT4 in C4-2B cells. Treatment of C4-2B abiraterone-resistance and C4-2B parental cells with a combination of abiraterone plus ICG001 resulted in a marked decrease in AR and its downstream targets PSA and CDC20 after 24 h exposure, compared to untreated cells. Abiraterone or ICG001 individually in C4-2B parental cells showed a modest change in the protein expression of these molecules. Expression levels of  $\beta$ -catenin, c-Myc, and cyclin D1 levels were decreased in C4-2B abiraterone-resistant cells after 24 h of treatment individually with ICG001, compared to untreated cells. In addition, combination of abiraterone plus ICG001 resulted in

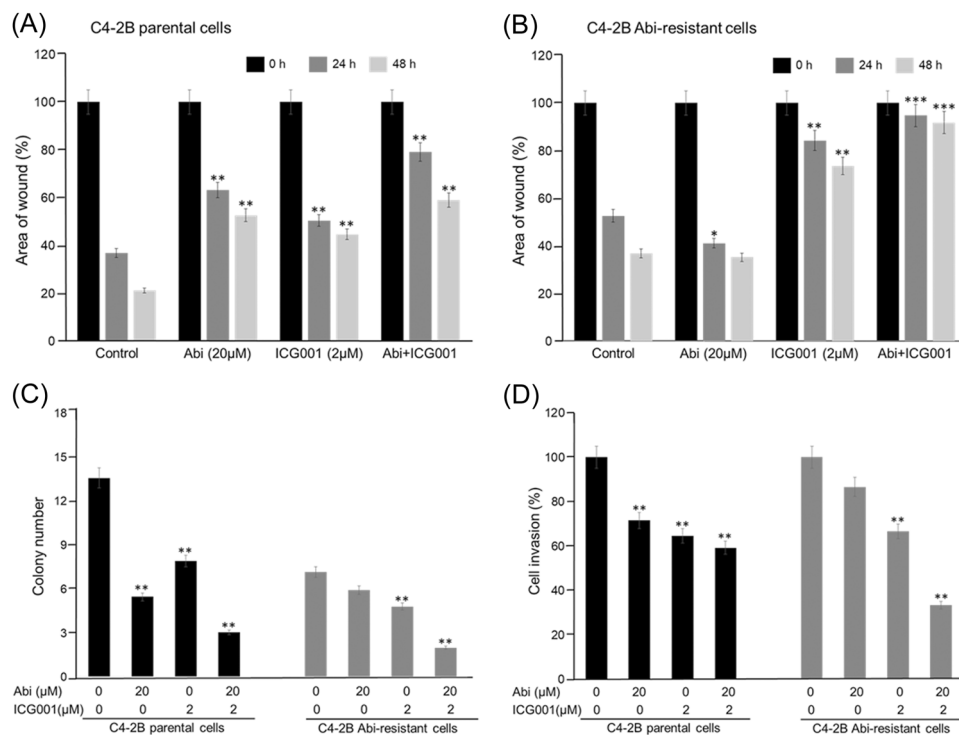


**FIGURE 5** Effect of ICG001 and abiraterone alone or in combination on migration potential in (A) C4-2B parental cells, and (B) C4-2B abiraterone-resistant cells. The cells were treated with 2  $\mu$ M ICG001 or 20  $\mu$ M abiraterone acetate alone and in combination and wound healing assay was performed. Results are expressed as percentage area of wound where the remaining area determined by normalizing the area of wound after 24 or 48 h, as indicated, to the initial wound area at 0 h (set to 100%). Each bar represents the mean of three to five fields measured  $\pm$  SD. (C) Colony formation assay and (D) Cell invasion assay. Results were expressed as the percentage of the invading cells at 48 h or difference in absorbance at 480 nm. Each bar represents the mean of 3 to 5 fields measured  $\pm$  SD. Two-tailed Student *t* test was used to compare treatment groups and control. \**p* < 0.05, \*\**p* < 0.01, \*\*\**p* < 0.001 versus control. Details are provided in Section 2.

decreased expression of stem cell markers ALDH1, SOX2, and OCT4 in both C4-2B abiraterone-resistant and C4-2B parental cells following 24 h exposure. A combination of abiraterone plus ICG001 demonstrates a marked and sustained inhibition of PCNA, a cell proliferation marker, compared to individual treatment and the corresponding untreated group (Figure 6A).

In prostate cancer,  $\beta$ -catenin binds AR through direct occupancy at its promoter.<sup>34,35</sup> In fact,  $\beta$ -catenin and SOX9 complex, interacts and physically associate with AR.<sup>36,37</sup> Therefore, we next determine the effect of abiraterone and ICG001 on disruption of AR binding with the  $\beta$ -catenin and SOX9 complex. Immunoprecipitation experiments were performed in C4-2B abiraterone-resistant and C4-2B parental cells pulling down AR in these samples and probing for  $\beta$ -catenin and SOX9 in the complex. The immunoprecipitation data confirmed the association between AR and  $\beta$ -catenin/SOX9 complex. While the individual treatments with ICG001 and abiraterone did not markedly affect the association, the combination treatment abrogated the association between AR and the  $\beta$ -catenin and SOX9 from the complex more prominently in C4-2B abiraterone-resistant cells (Figure 6B).

To validate the synergistic effect of abiraterone and ICG001 in the inhibition of tumor growth, we employed C4-2B abiraterone-resistant tumor xenograft model. Individual

treatment with abiraterone or ICG001 partially suppressed tumor growth, but the inhibitory effect was much stronger with the combination of abiraterone plus ICG001 (Figure 7A). No significant side effect was observed as only a modest change in the body weight was noted (data not shown). Although both wet weight and size of the tumors were reduced with monotherapy of abiraterone or ICG001, the effect was much more significant with the combination treatment (Figure 7B). Immunoblotting for PCNA confirmed that tumors after combination therapy had a significant reduction in overall proliferation. Although individual treatment with abiraterone or ICG001 decreased the expression of AR, c-Myc, cyclin D1; and  $\beta$ -catenin, a more significant decrease in the expression of these proteins was observed in the combined treatment. Finally, PSA and CDC20 expression were also decreased upon combination treatment compared with individual treatments, an indication of the inhibition of AR activity. In addition, a significant decrease in the expression of stem cell markers viz. ALDH1, SOX2, and OCT4 was observed in the combination treatment, compared to individual treatments and the vehicle control. ICG001 reduced  $\beta$ -catenin level but not abiraterone treatment. Combination treatment of abiraterone and ICG001 showed marked inhibition on  $\beta$ -catenin expression in the tumor specimens (Figure 7C).

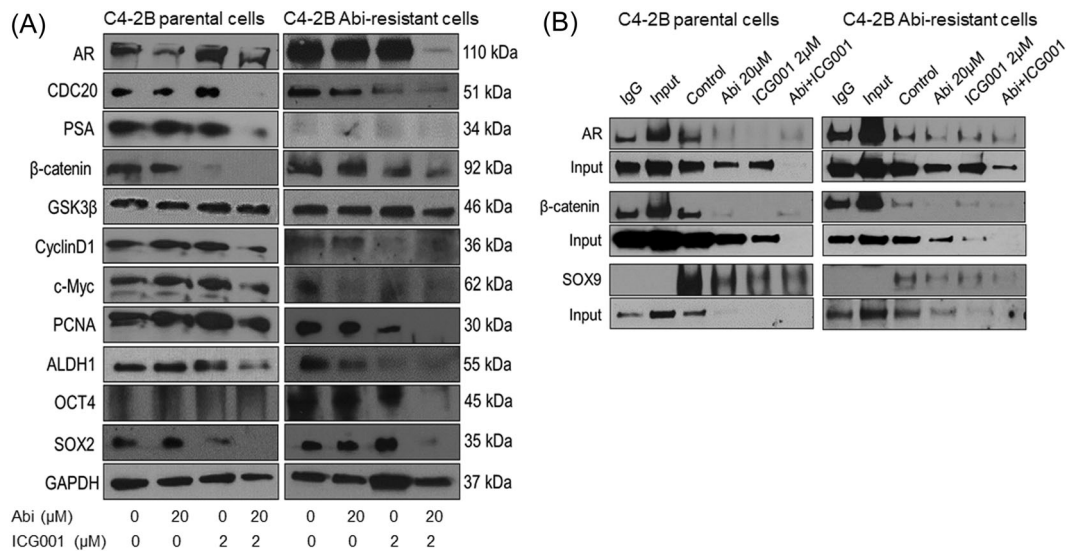


**FIGURE 6** (A) Effect of ICG001 and abiraterone alone or in combination on the protein expression of AR and β-catenin signaling and their downstream targets including CDC20, PSA, GSK3β, Cyclin D1, c-Myc, PCNA and stem cell targets ALDH1, OCT4, and SOX2 expression in C4-2B parental and C4-2B abiraterone resistant cells. The cells treated with 2 μM ICG001 or 20 μM abiraterone acetate alone and in combination and Western blotting was performed. GAPDH as loading control. (B) Immunoprecipitation in C4-2B abiraterone resistant and C4-2B parental cells pulling down AR in these samples and probe for β-catenin/SOX9 in the complex. The inputs are provided in separate blots. Details are provided in Section 2.

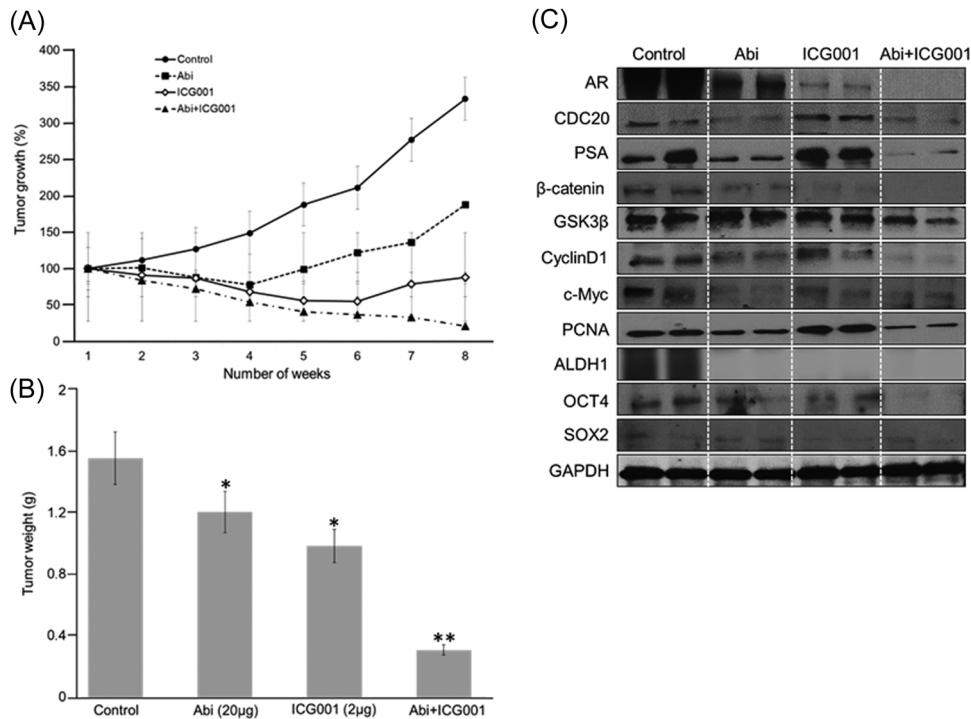


**FIGURE 7** Effect of ICG001 and abiraterone alone or in combination on C4-2B abiraterone resistant tumor growth in athymic nude mice and its correlation with downregulation of β-catenin and AR signaling pathway. (A) Tumor growth (%) in control and treated groups, (B) Wet weight of tumors is represented as the mean of 4–6 tumors from each group. Values are means ± SD, n = 4–6 tumors. \*p < 0.05 and \*\*p < 0.001 versus control. (C) Western blotting for AR, CDC20, PSA, β-catenin, GSK3β, cyclin D1, c-Myc, PCNA, ALDH1, OCT4, and SOX2 in tumor lysates in control and treated groups at the indicated concentration. The blots were stripped and reprobbed with anti-GAPDH antibody to ensure equal protein loading. Details are provided in Section 2.



## 4 | DISCUSSION

Androgen deprivation therapy (ADT) with the use of androgen signaling inhibitors including abiraterone acetate has exhibited improved overall survival in prostate cancer patients by several months.<sup>1,38</sup> Unfortunately, despite the demonstrated benefit, not all patients respond to treatment and almost all are destined to develop a resistant phenotype with the emergence of castration-resistant prostate cancer (CRPC) phenotype.<sup>39,40</sup> Enough evidence supports the notion that higher expression of androgen receptor (AR) along with alterations in various signaling pathways might be the possible reason for abiraterone resistance.<sup>39,40</sup> Number of studies have described the physical and functional interaction of AR and  $\beta$ -catenin.<sup>17,18</sup> This phenomenon provides a significant rationale to target  $\beta$ -catenin and AR in CRPC tumors. As individual agents, AR inhibitors or  $\beta$ -catenin is not highly effective and result in therapeutic resistance as a consequence of the reciprocal feedback activation loop and emergence of AR splice variants. Our analysis revealed that overexpression of both canonical Wnt/ $\beta$ -catenin signaling and noncanonical Wnt pathways are associated with abiraterone resistance and that combined treatment of abiraterone and ICG001 is highly effective treatment strategy.

Gain of function of the AR, and  $\beta$ -catenin overexpression correlate with metastatic progression to advance-stage disease.<sup>6-8</sup> It has been demonstrated that  $\beta$ -catenin functions as a transcriptional coactivator with AR in CRPC tumors.<sup>9,10</sup> More recent evidence suggests that the Wnt signaling pathway plays a role in prostate cancer progression to an AR-indifferent or neuroendocrine phenotype where the Wnt secretion mediator, Wntless is recognized as a major driver of neuroendocrine-differentiated prostate cancer characterized by aggressive tumor growth.<sup>41,42</sup> These CRPC-Wnt tumors express minimal to low expression of AR and reduced PSA levels. These studies highlight another subtype of CRPC tumors and provide a rationale for targeting with the therapeutic molecules of Wnt signaling pathway for its treatment.

The noncanonical Wnt signaling utilizes  $\beta$ -catenin-independent pathway stimulating a transcriptional response.<sup>11-13</sup> Human non-canonical Wnt ligands Wnt5A, Wnt5B, and Wnt11 transduce planar cell polarity signals through the Frizzled receptors and the co-receptors ROR1, ROR2, or RYK stimulating invasion and metastasis in malignant cells.<sup>12,13</sup> A study on a single cell RNA sequencing of circulating tumor cells from patients with metastatic prostate cancer exhibited upregulation of noncanonical Wnt signaling in abiraterone-treated patients.<sup>7</sup> Another study of prostate cancer patients with bone metastasis receiving androgen deprivation therapy demonstrated expression of bone morphogenetic protein-6 induced by Wnt5A, suggesting noncanonical Wnt signaling as a potential mechanism for castration resistance.<sup>8</sup> Our transcriptomics data showed significant increase in WNT5A together with overrepresentation of noncanonical Wnt signaling in C4-2B abiraterone-resistant cells. Although the present work focuses on the role of canonical Wnt signaling, however additional studies are required to determine

whether suppression of the noncanonical Wnt pathway might acquire benefit from androgen deprivation therapy.

Accumulating data suggest that small subpopulations of cancer cells, termed as cancer stem cells (CSCs) possess ability to self-renew as well as differentiate to a daughter cell type, play a critical role in both initiation and maintenance of tumors.<sup>32,33</sup> It has been suggested that these cells are resistant to conventional chemotherapy and radiation, making it important to develop therapeutic approaches to selectively target them, perhaps by interfering with cell-specific signaling pathways that regulate self-renewal. In prostate cancer, it is possible that CSCs survive after ADT, causing CRPC expansion.<sup>43,44</sup> Growing evidence suggest that Wnt/ $\beta$ -catenin signaling is highly active in CRPC and may have a role in CSC differentiation and self-renewal.<sup>45,46</sup> Our data support the idea that combined treatment with abiraterone and ICG001 decreases CSC differentiation and their markers including ALDH1, SOX2, and OCT4 which correlate with colony formation ability.

The transcription factor SOX9 has been shown to upregulate multiple components of the Wnt/ $\beta$ -catenin pathway suggesting a potential mechanism for the reactivation. Crosstalk between Wnt/ $\beta$ -catenin and SOX9 increases AR transcription which leads to the synergistic aberrant expression of target genes involved in the emergence of CRPC.<sup>19,20</sup> Many Wnt-dependent CRPC cell lines and primary CRPC tumors show high levels of SOX9 expression, and recent reports also suggest that SOX9 promotes CRPC stemness and survival.<sup>36</sup> The co-immunoprecipitation studies confirmed that SOX9 and  $\beta$ -catenin form a physical complex. In our study, we immunoprecipitated AR and  $\beta$ -catenin in C4-2B abiraterone-resistant and parental cell line and probe for SOX9 association. Our studies demonstrate that combination treatment with abiraterone and ICG001 abrogates the association between AR and  $\beta$ -catenin and inhibits SOX9 expression. This signifies that combined targeting of AR and  $\beta$ -catenin is an effective strategy for CRPC treatment.

Reports suggest that androgens remain the critical driver of cell cycle progression in cancer primarily through G1-S phase transition. Mechanistic investigations have highlighted that AR regulates several cell cycle regulatory genes including cyclins and cyclin dependent kinases to induce signals that promote cell cycle governing androgen-dependent proliferation.<sup>45</sup> Previous studies have demonstrated that levels of cyclin D1 isoforms are elevated in CRPC and selectively manipulate AR signaling to promote metastatic phenotypes.<sup>47,48</sup> Similarly, our results indicate that inhibition of AR by abiraterone blocked CRPC cells entering into the S-phase from G1 of the cell cycle. Interestingly,  $\beta$ -catenin also contributes to cell cycle regulation in various human cancers.<sup>48</sup> Wnt/ $\beta$ -catenin upregulation increases  $\beta$ -catenin in the nucleus that leads to activation of the expression of cyclin D1 and c-Myc, where the former influences the G1 phase of the cell division cycle, and the latter, the S phase.<sup>49,50</sup> Our studies further demonstrate that the combination of abiraterone plus ICG001 was highly effective in arresting abiraterone-resistant cells in the G0/G1-phase cell cycle arrest compared to their individual treatments.<sup>51</sup>

In summary, our data provide a potential mechanism of progression to CRPC that involves aberrant expression of members of the canonical Wnt/ $\beta$ -catenin pathway, which promotes the interaction between AR and  $\beta$ -catenin and thereby increases the transactivation of the AR to initiate transcription of genes normally regulated by androgens. Aberrant activation of the AR through the Wnt/ $\beta$ -catenin signaling pathway plays a key role in the progression of prostate cancer to the castrate-resistant stage. This opens a new therapeutic opportunity for the management of CRPC patients.

## AUTHOR CONTRIBUTIONS

**Eswar Shankar:** Conceptualization; methodology; software; formal analysis; visualization. **Sanjay Gupta:** Conceptualization; formal analysis; data curation; writing—original draft preparation; writing—review & editing; visualization; supervision; project administration; funding acquisition. **Ibrahim M. Atawia:** Methodology; validation; formal analysis; funding acquisition. **Prem P. Kushwaha:** Methodology; software; validation; validation; formal analysis; writing—original draft preparation; writing—review & editing. **Shiv Verma:** Methodology; validation; formal analysis; data curation; writing—original draft preparation; writing—review & editing. **Spencer Lin:** Methodology. **Osama Abdel-Gawad:** Writing—review & editing; visualization.

## ACKNOWLEDGMENTS

The authors are thankful to the Genomics Core Facility of the CWRU School of Medicine's Genetics and Genome Sciences Department for performing Next-Gen sequencing and Ms. Simone Edelheit for technical assistance. Efforts are supported by the Department of Defense Grants W81XWH-19-1-0720 and W81XWH-18-1-0618 to SG.

## CONFLICT OF INTEREST STATEMENT

The authors declare no conflict of interest.

## DATA AVAILABILITY STATEMENT

The data that support the findings of this study are available from the corresponding author upon reasonable request.

## ORCID

Sanjay Gupta  <http://orcid.org/0000-0002-9492-3249>

## REFERENCES

- Fizazi K, Tran N, Fein L, et al. Abiraterone plus prednisone in metastatic, castration-sensitive prostate cancer. *N Engl J Med*. 2017;377(4):352-360.
- Duarte C, Jimeno A, Kessler ER. Abiraterone acetate to treat metastatic castration-resistant prostate cancer in combination with prednisone. *Drugs Today*. 2019;55(1):5-15.
- Cheong EJY, Nair PC, Neo RWY, et al. Slow-, tight-binding inhibition of CYP17A1 by abiraterone redefines its kinetic selectivity and dosing regimen. *J Pharmacol Exp Ther*. 2020;374(3):438-451.
- Rydzewska LHM, Burdett S, Vale CL, et al. Adding abiraterone to androgen deprivation therapy in men with metastatic hormone-sensitive prostate cancer: a systematic review and meta-analysis. *Eur J Cancer*. 2017;84:88-101.
- Caffo O, Veccia A, Kinspergher S, Maines F. Abiraterone acetate and its use in the treatment of metastatic prostate cancer: a review. *Future Oncol*. 2018;14(5):431-442.
- Wang L, Dehm SM, Hillman DW, et al. A prospective genome-wide study of prostate cancer metastases reveals association of wnt pathway activation and increased cell cycle proliferation with primary resistance to abiraterone acetate-prednisone. *Ann Oncol*. 2018;29(2):352-360.
- Miyamoto DT, Zheng Y, Wittner BS, et al. RNA-Seq of single prostate CTCs implicates noncanonical Wnt signaling in antiandrogen resistance. *Science*. 2015;349(6254):1351-1356.
- Annala M, Vandekerckhove G, Khalaf D, et al. Circulating tumor DNA genomics correlate with resistance to abiraterone and enzalutamide in prostate cancer. *Cancer Discov*. 2018;8(4):444-457.
- Zhan T, Rindtorff N, Boutros M. Wnt signaling in cancer. *Oncogene*. 2017;36(11):1461-1473.
- Zhang Y, Zu D, Chen Z, Ying G. An update on Wnt signaling pathway in cancer. *Transl Cancer Res*. 2020;9(2):1246-1252.
- Menck K, Heinrichs S, Baden C, Bleckmann A. The WNT/ROR pathway in cancer: from signaling to therapeutic intervention. *Cells*. 2021;10(1):142.
- Asem M, Buechler S, Wates R, Miller D, Stack M. Wnt5a signaling in cancer. *Cancers*. 2016;8(9):79.
- Koushyar S, Grant GH, Uysal-Onganer P. The interaction of Wnt-11 and signalling cascades in prostate cancer. *Tumor Biol*. 2016;37(10):13049-13057.
- Krishnamurthy N, Kurzrock R. Targeting the wnt/beta-catenin pathway in cancer: update on effectors and inhibitors. *Cancer Treat Rev*. 2018;62:50-60.
- Yokoyama NN, Shao S, Hoang BH, Mercola D, Zi X. Wnt signaling in castration-resistant prostate cancer: implications for therapy. *Am J Clin Exp Urol*. 2014;2(1):27-44.
- Wang G, Wang J, Sadar MD. Crosstalk between the androgen receptor and  $\beta$ -catenin in castrate-resistant prostate cancer. *Cancer Res*. 2008;68(23):9918-9927.
- Beildeck ME, Gelmann EP, Byers W. Cross-regulation of signaling pathways: an example of nuclear hormone receptors and the canonical Wnt pathway. *Exp Cell Res*. 2010;316(11):1763-1772.
- Schweizer L, Rizzo CA, Spires TE, et al. The androgen receptor can signal through Wnt/ $\beta$ -Catenin in prostate cancer cells as an adaptation mechanism to castration levels of androgens. *BMC Cell Biol*. 2008;9:4.
- Ma F, Ye H, He HH, et al. SOX9 drives WNT pathway activation in prostate cancer. *J Clin Invest*. 2016;126(5):1745-1758.
- Khurana N, Sikka SC. Interplay between SOX9, Wnt/ $\beta$ -catenin and androgen receptor signaling in castration-resistant prostate cancer. *Int J Mol Sci*. 2019;20(9):2066.
- Veldscholte J, Berrevoets CA, Ris-Stalpers C, et al. The androgen receptor in LNCaP cells contains a mutation in the ligand binding domain which affects steroid binding characteristics and response to antiandrogens. *J Steroid Biochem Mol Biol*. 1992;41(3-8):665-669.
- Spans L, Helsen C, Clinckemalie L, et al. Comparative genomic and transcriptomic analyses of LNCaP and C4-2B prostate cancer cell lines. *PLoS ONE*. 2014;9(2):e90002.
- Verma S, Shankar E, Kalayci FNC, et al. Androgen deprivation induces transcriptional reprogramming in prostate cancer cells to develop stem cell-like characteristics. *Int J Mol Sci*. 2020;21(24):9568.
- Liberzon A, Birger C, Thorvaldsdóttir H, Ghandi M, Mesirov JP, Tamayo P. The molecular signatures database hallmark gene set collection. *Cell Systems*. 2015;1(6):417-425.
- Shankar E, Franco D, Iqbal O, Moreton S, Kanwal R, Gupta S. Dual targeting of EZH2 and androgen receptor as a novel therapy for castration-resistant prostate cancer. *Toxicol Appl Pharmacol*. 2020;404:115200.



26. Singh U, Quintanilla RH, Grecian S, Gee KR, Rao MS, Lakshminpathy U. Novel live alkaline phosphatase substrate for identification of pluripotent stem cells. *Stem Cell Rev Rep*. 2012;8(3):1021-1029.
27. Lu HE, Tsai MS, Yang YC, et al. Selection of alkaline phosphatase-positive induced pluripotent stem cells from human amniotic fluid-derived cells by feeder-free system. *Exp Cell Res*. 2011;317(13):1895-1903.
28. Lee E, Ha S, Logan SK. Divergent androgen receptor and beta-catenin signaling in prostate cancer cells. *PLoS One*. 2015;10(10):e0141589.
29. Lee SH, Luong R, Johnson DT, et al. Androgen signaling is a confounding factor for  $\beta$ -catenin-mediated prostate tumorigenesis. *Oncogene*. 2016;35(6):702-714.
30. Patel R, Brzezinska EA, Repiscak P, et al. Activation of  $\beta$ -catenin cooperates with loss of Pten to drive AR-independent castration-resistant prostate cancer. *Cancer Res*. 2020;80(3):576-590.
31. Borowicz S, Van Scoyk M, Avasarala S, et al. The soft agar colony formation assay. *J Vis Exp*. 2014;92:e51998.
32. Huang H, Wang C, Liu F, et al. Reciprocal network between cancer stem-like cells and macrophages facilitates the progression and androgen deprivation therapy resistance of prostate cancer. *Clin Cancer Res*. 2018;24(18):4612-4626.
33. Yang X, Chen MW, Terry S, et al. Complex regulation of human androgen receptor expression by Wnt signaling in prostate cancer cells. *Oncogene*. 2006;25(24):3436-3444.
34. Lee E, Madar A, David G, Garabedian MJ, Dasgupta R, Logan SK. Inhibition of androgen receptor and  $\beta$ -catenin activity in prostate cancer. *Proc Natl Acad Sci*. 2013;110(39):15710-15715.
35. Chesire DR, Isaacs WB. Ligand-dependent inhibition of  $\beta$ -catenin/TCF signaling by androgen receptor. *Oncogene*. 2002;21(55):8453-8469.
36. Wang H, McKnight NC, Zhang T, Lu ML, Balk SP, Yuan X. SOX9 is expressed in normal prostate basal cells and regulates androgen receptor expression in prostate cancer cells. *Cancer Res*. 2007;67(2):528-536.
37. Schneider JA, Logan SK. Revisiting the role of Wnt/ $\beta$ -catenin signaling in prostate cancer. *Mol Cell Endocrinol*. 2018;462:3-8.
38. de Bono JS, Logothetis CJ, Molina A, et al. Abiraterone and increased survival in metastatic prostate cancer. *N Engl J Med*. 2011;364(21):1995-2005.
39. Annala M, Taavitsainen S, Khalaf DJ, et al. Evolution of castration-resistant prostate cancer in ctDNA during sequential androgen receptor pathway inhibition. *Clin Cancer Res*. 2021;27(16):4610-4623.
40. Lorente D, De Bono JS. Molecular alterations and emerging targets in castration resistant prostate cancer. *Eur J Cancer*. 2014;50(4):753-764.
41. Bland T, Wang J, Yin L, et al. WLS-Wnt signaling promotes neuroendocrine prostate cancer. *iScience*. 2021;24(1):101970.
42. Tang F, Xu D, Wang S, et al. Chromatin profiles classify castration-resistant prostate cancers suggesting therapeutic targets. *Science*. 2022;376(6596):eabe1505.
43. Jamroze A, Chatta G, Tang DG. Androgen receptor (AR) heterogeneity in prostate cancer and therapy resistance. *Cancer Lett*. 2021;518:1-9.
44. Harris KS, Kerr BA. Prostate cancer stem cell markers drive progression, therapeutic resistance, and bone metastasis. *Stem Cells Int*. 2017;2017:1-9.
45. Yeh Y, Guo Q, Connelly Z, et al. Wnt/ $\beta$ -catenin signaling and prostate cancer therapy resistance. *Adv Exp Med Biol*. 2019;1210:351-378.
46. Katoh M. Canonical and non-canonical WNT signaling in cancer stem cells and their niches: cellular heterogeneity, omics reprogramming, targeted therapy and tumor plasticity. *Int J Oncol*. 2017;51(5):1357-1369.
47. Schiewer MJ, Morey LM, Burd CJ, et al. Cyclin D1 repressor domain mediates proliferation and survival in prostate cancer. *Oncogene*. 2009;28(7):1016-1027.
48. Qie S, Diehl JA. Cyclin D1, cancer progression, and opportunities in cancer treatment. *J Mol Med*. 2016;94(12):1313-1326.
49. Shukla S, MacLennan GT, Flask CA, et al. Blockade of  $\beta$ -catenin signaling by plant flavonoid apigenin suppresses prostate carcinogenesis in TRAMP mice. *Cancer Res*. 2007;67(14):6925-6935.
50. Shang S, Hua F, Hu ZW. The regulation of  $\beta$ -catenin activity and function in cancer: therapeutic opportunities. *Oncotarget*. 2017;8(20):33972-33989.
51. Cifuentes E, Croxen R, Menon M, Barrack ER, Reddy GPV. Synchronized prostate cancer cells for studying androgen regulated events in cell cycle progression from G1 into S phase. *J Cell Physiol*. 2003;195(3):337-345.

## SUPPORTING INFORMATION

Additional supporting information can be found online in the Supporting Information section at the end of this article.

**How to cite this article:** Atawia IM, Kushwaha PP, Verma S, et al. Inhibition of Wnt/ $\beta$ -catenin pathway overcomes therapeutic resistance to abiraterone in castration-resistant prostate cancer. *Molecular Carcinogenesis*. 2023;62:1312-1324. doi:10.1002/mc.23565